Isospin effect in statistical sequential decay

W. D. Tian,* Y. G. Ma, X. Z. Cai, D. Q. Fang, W. Guo, W. Q. Shen, K. Wang, and H. W. Wang
Shanghai Institute of Applied Physics, Chinese Academy of Sciences, P. O. Box 800-204, 201800 Shanghai, People's Republic of China

M. Veselsky
Institute of Physics, Slovak Academy of Sciences, Dubravska cesta 9, Bratislava, Slovakia
(Received 4 February 2007; revised manuscript received 6 July 2007; published 23 August 2007)

Isospin effect of the statistical emission fragments from the equilibrated source is investigated in the frame of statistical binary decay implemented into the GEMINI code, isoscaling behavior is observed and the dependences of isoscaling parameters α and β on emission fragment size, source size, source isospin asymmetry and excitation energies are studied. Results show that α and β neither depends on light fragment size nor on source size. A good linear dependence of α and β on the inverse of temperature T is manifested and the relationship of $\alpha = 4C_{sym}[(Z_s/A_s)_1^2 - (Z_s/A_s)_2^2]/T$ and $\beta = 4C_{sym}[(N_s/A_s)_1^2 - (N_s/A_s)_2^2]/T$ from different isospin asymmetry sources is satisfied. The symmetry energy coefficient C_{sym} extracted from simulation results is ~ 23 MeV which includes both the volume and surface term contributions, of which the surface effect seems to play a significant role in the symmetry energy.

DOI: 10.1103/PhysRevC.76.024607 PACS number(s): 24.10.Pa, 24.60.Dr, 25.70.−z

I. INTRODUCTION

The growing interest in isospin effects in nuclear reactions is motivated by an increasing awareness of the importance of the symmetry term in the nuclear equation of state. The availability of beams with large neutron-to-proton ratio, N/Z, provides the opportunity to explore the symmetry energy in very isospin-asymmetric nuclear systems. In such reactions, isospin degree of freedom has a prominent role and can serve as a valuable probe of the symmetry energy term of the nuclear equation of state. The isotopic composition of the nuclear reaction products contains important information on the role of the isospin on the reaction process. N/Z degree of freedom and its equilibration, as well as the isospin asymmetry dependent terms of the nuclear equation of state (EOS) [1–6], has motivated detailed measurements of the isotopic distributions of reaction products.

One important observable in heavy-ion collisions for determining the symmetry energy experimentally is the fragment isotopic composition investigated with the recently developed isoscaling approach [7,8]. The isoscaling approach attempts to isolate the effects of the nuclear symmetry energy in the fragment yields, thus allowing a direct study of the symmetry energy term in the nuclear binding energy during formation of hot fragments. Isoscaling refers to a general exponential relation between the yield ratios of given fragments between two reactions which differ only in their isospin asymmetry (N/Z). In particular, if two reactions, 1 and 2, lead to primary fragments having approximately the same temperature but different isospin asymmetry, the ratio $R_{21}(N, Z)$ of the yields of a given fragment (N, Z) from these primary fragments exhibits an exponential dependence on the neutron number N and the atomic number Z by the following form:

$$R_2(N, Z) = \frac{Y_2(N, Z)}{Y_1(N, Z)} = C \exp(\alpha N + \beta Z), \qquad (1)$$

where α and β are two scaling parameters and C is an overall normalization constant. This scaling behavior has been observed in a very broad range of reactions [9–18] and theoretical calculations [19–31]. A review paper can be found in the recent international *World Consensus Initiative* book on "Dynamics and Thermodynamics with Nuclear Degrees of Freedom" [32].

The aim of the present paper is to investigate the isospin effect in sequential binary decay implemented into the GEMINI code by isolating formation of the excited composite system, to learn the sensitivity of the isoscaling parameters with respect to the observable characterizing the source's state by only observing the first step decayed fragments, such as N/Z distribution and isotopic characteristics of the evaporated light particle. The sequential binary decay model GEMINI [33–35] has been successfully used to describe the light particle evaporation, complex fragment emission, and N/Z distribution of the equilibrated compound source.

The article is organized as follows. Section II makes a simple review on the sequential binary decay implemented into the GEMINI code, where a brief description of the symmetry energy adopted in the binding energy calculation and the method to extract temperature are given. In Sec. III, isoscaling phenomenon and its dependence on compound source size, excitation energy and isospin asymmetry are presented, the sensitivities of the isoscaling parameters α and β to observables characterizing the state of the source are discussed in detail. The contribution from surface effect on the symmetry energy term is discussed in Sec. IV. Finally a summary is given.

*tianwendong@sinap.ac.cn

II. MODEL OVERVIEW

The GEMINI model [33,34] calculates the decay of compound nuclei by modes of sequential binary decays. All possible binary divisions from light-particle emission to symmetric division are considered. The model employs a Monte Carlo technique to follow the decay chains of individual compound nuclei through sequential binary decays until the resulting products are unable to undergo further decay.

The decay width for the evaporation of fragments with $Z \leqslant 2$ is calculated using the Hauser-Feshbach formalism [36]. For the emission of a light particle (Z_1, A_1) with spin J_1 from a system (Z_0, A_0) with excitation energy E^* and spin J_0, leaving the residual system Z_2, A_2 with spin J_2, the decay width is given by

$$\Gamma(Z_1, A_1, Z_2, A_2) = \frac{2J_1+1}{2\pi\rho_0} \sum_{l=|J_0-J_2|}^{J_0+J_2} \int_0^{E^*-B-E_{rot}(J_2)} T_l(\varepsilon)\rho_2(U_2, J_2)d\varepsilon. \quad (2)$$

In this equation l and ε are the orbital angular momentum and kinetic energy of the emitted particle, $\rho_2(U_2, J_2)$ is the level density of the residual system with thermal excitation energy

$$U_2 = E^* - B - E_{rot}(J_2) - \varepsilon, \quad (3)$$

where B is the binding energy, $E_{rot}(J_2)$ is the rotation plus deformation energy of the residual system, ρ_0 is level density of the initial system, and T_l is the transmission coefficients.

For binary divisions corresponding to the emission of a heavier fragment, the decay width is calculated using the transition state formalism of Moretto [37]

$$\Gamma(Z_1, A_1, Z_2, A_2) = \frac{1}{2\pi\rho_0} \int_0^{E^*-E_{sad}(J_0)} \rho_{sad}(U_{sad}, J_0)d\varepsilon, \quad (4)$$

where U_{sad} and ρ_{sad} are the thermal energy and level density of the conditional saddle-point configuration, respectively,

$$U_{sad} = E^* - E_{sad}(J_0) - \varepsilon, \quad (5)$$

where E_{sad} is the deformation plus rotation energy of the saddle-point configuration and ε now is the kinetic energy of the translational degree of freedom.

The symmetry energy term due to the neutron-proton excess is presented in calculating the masses of nuclei. For heavy systems ($Z > 12$), the masses of the initial and residual systems are obtained from the Yukawa-plus-exponential model of Krappe, Nix, and Sierk [38] without the shell correction, the pairing correction term for odd-odd nuclei is included. The parameters for this model are taken from the fit to experimental masses of Möller and Nix [39]. For very light systems ($A \leqslant 12$), masses of the nuclei are calculated from the experimental ones.

Taking into account the effect of a predicted increase in the symmetry energy associated with the temperature dependence of effective nucleon mass in the surface of the nucleus [41], the kinetic part of the symmetry energy is related to the level spacing at the Fermi surface and so it is also related to the level density parameter a_T, the following temperature-dependent kinetic symmetry energy was therefore included to calculate the temperature dependent level density parameter a_T in the GEMINI simulations [35,40]

$$E_{sym}^{kin}(T) = 0.82247\left(\frac{1}{a_T} - \frac{1}{a_0}\right)(N-Z)^2, \quad (6)$$

where $a_0 = (1.6A + 1.8A^{2/3})/15.5$.

The effective thermal excitation energy of the equilibrated system before light particle evaporation and saddle-point configuration before heavy fragment emission can be obtained by

$$E_{ex}^{ther} = U_2 - E_{sym}^{kin}, \quad (7)$$

or

$$E_{ex}^{ther} = U_{sad} - E_{sym}^{kin}. \quad (8)$$

Then the nuclear system temperature is approximately

$$T = \sqrt{E_{ex}^{ther}/a_T}. \quad (9)$$

III. ISOSCALING BEHAVIORS

To make a systematic study of source parameters which might influence the isoscaling behavior, in our present work several pairs of equilibrated sources are considered at various initial excitation energies $E_{ex} = 1.0$, 1.4, 2.0, 2.4, and 3.0 MeV/nucleon. To avoid possible effects of different magnitudes of Coulomb interaction on isotopic distributions, we consider pairs of sources with the same proton numbers Z_s but different mass numbers A_s. The equilibrated source pairs are chosen at different mass region and system isospin asymmetry N/Z, two groups of the source pairs have been used: (1) $Z_s = 50$ with $A_s = 100$, 105, 110, and 115, respectively; (2) $Z_s = 30$ with $A_s = 60$, 63, 66, and 69, respectively. We adopt the widely used convention to denote with the index "2" the more neutron-rich system and with the index "1" the more neutron-poor system. In this situation the value of α is always positive because more neutron-rich clusters will be produced by the neutron-richer source and the value of β is always negative. The yield ratios $R_{21}(N, Z)$ are calculated and the corresponding isoscaling behaviors are investigated over all possible decayed fragments. In the present study, we will focus on the first decay step to investigate the decay products even though a real decay chain is usually longer than one for the deexcitation process of a thermal source. The advantage of studies on the first step is that the source size and temperature parameters are well defined.

Figure 1 plots the isoscaling parameters α and β as a function of fragment proton number Z and neutron number N for source pairs with fixed proton number: [$Z_s = 50$, $A_s = 100$ ($N_s/Z_s = 1.0$) and $A_s = 105$ ($N_s/Z_s = 1.1$)] at excitation energies 1.0, 1.4, 2.0, 2.4, and 3.0 MeV/nucleon. Figures 2 and 3 plot the isoscaling parameters α and β as a function of fragment proton number Z and neutron number N for different size source pairs at excitation energies 2.0 MeV/nucelon, respectively. Figure 2 shows the source pairs with source atomic number $Z_s = 50$ and different mass number $A_s = 100$, 105, 110, and 115, and Fig. 3 is for the source pairs with source

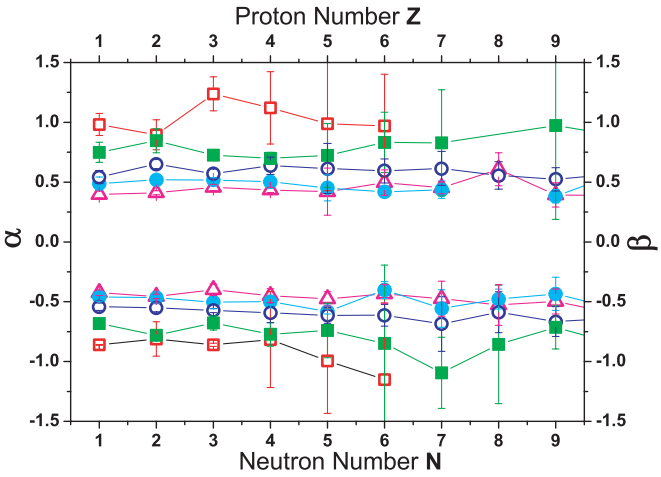

FIG. 1. (Color online) Isoscaling parameters α (positive values) and β (negative values) as a function of the fragment proton number Z or neutron number N from source pair ($Z_s = 50$, $A_s = 100$) and ($Z_s = 50$, $A_s = 105$) at various excitation energies: $E_{ex} = 1.0$ (open squares), 1.4 (solid squares), 2.0 (open circles), 2.4 (solid circles), 3.0 (open up triangles) MeV/nucleon.

atomic number $Z_s = 30$ and different mass number $A_s = 60$, 63, 66, and 69.

Figures 1, 2, and 3 show that the values of isoscaling parameters α and β are essentially flat with the fragment proton number Z or neutron number N in the case plotted, as well as cases which included in the simulations which were not plotted in the figure samples. Average isoscaling parameters α and β can be calculated over the flat region to discuss the dependence of α and β on the properties of emission source, such as excitation energy, source size and source asymmetry of the isospin. The average α is calculated over the range $Z \leqslant 9$ and the average β is calculated over the range $N \leqslant 9$,

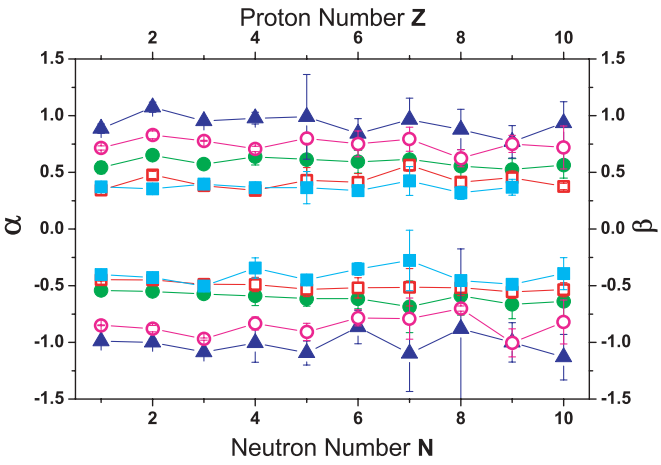

FIG. 2. (Color online) Isoscaling parameters α (positive values) and β (negative values) as a function of the fragment proton number Z or neutron number N from source pairs with the fixed proton number $Z_s = 50$ at excitation energies $E_{ex} = 2$ MeV/nucleon. Symbols in the figure correspond to $Y_{A_s=115}/Y_{A_s=110}$ (solid squares), $Y_{A_s=110}/Y_{A_s=105}$ (open squares), $Y_{A_s=105}/Y_{A_s=100}$ (solid circles), $Y_{A_s=115}/Y_{A_s=105}$ (open circles), $Y_{A_s=110}/Y_{A_s=100}$ (solid up triangles).

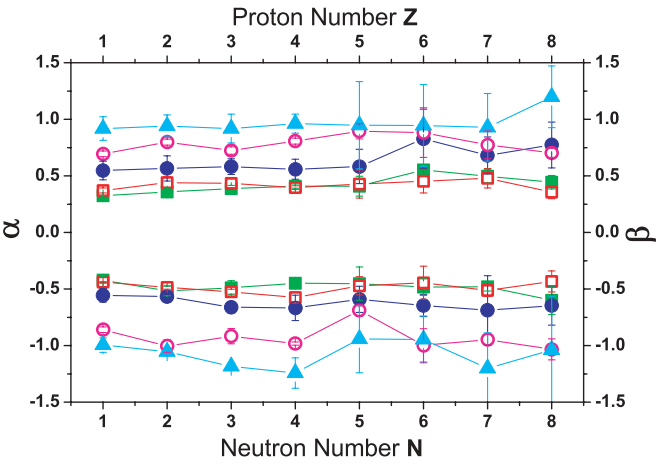

FIG. 3. (Color online) Same as Fig. 2, but for source pairs with the fixed proton number $Z_s = 30$ at excitation energies $E_{ex} = 2$ MeV/nucleon. Symbols in the figure correspond to $Y_{A_s=69}/Y_{A_s=66}$ (solid squares), $Y_{A_s=66}/Y_{A_s=63}$ (open squares), $Y_{A_s=63}/Y_{A_s=60}$ (solid circles), $Y_{A_s=69}/Y_{A_s=63}$ (open circles), $Y_{A_s=66}/Y_{A_s=60}$ (solid up triangles).

which keep both average values are calculated over on the same fragments region. In the following subsections isoscaling parameters α and β refer to the calculated average values.

A. Dependence of α and β on excitation energy

The excitation energy and temperature dependences of α and β are shown in Figs. 4 and 5 for different size and isospin asymmetry source pairs, respectively. Temperatures of the initial source are tabulated in Table I, in which the level density parameter a_T is derived from Eq. (6) and the temperature are calculated from Eq. (9).

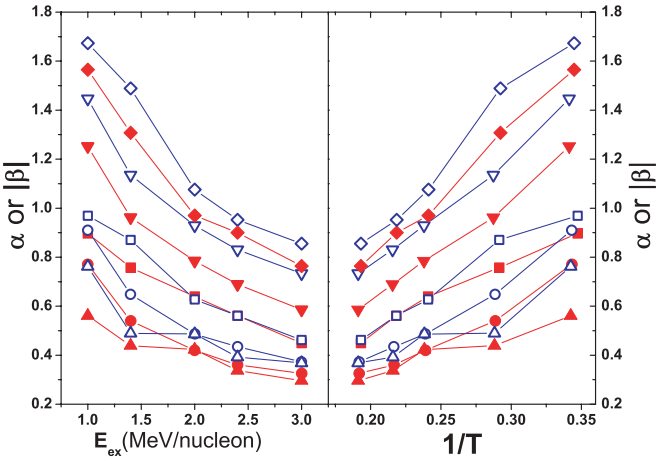

FIG. 4. (Color online) Dependence of isoscaling parameters α and $|\beta|$ on excitation energy (left panel) and the inverse temperature $1/T$ (right panel) for various source pairs with same proton number $Z_s = 30$. Symbols in the figure are α (solid symbols) or $|\beta|$ (open symbols) from source pair $Y_{A_s=63}/Y_{A_s=60}$ (squares), $Y_{A_s=66}/Y_{A_s=63}$ (circles), $Y_{A_s=69}/Y_{A_s=66}$ (up-triangles), $Y_{A_s=66}/Y_{A_s=60}$ (down-triangles), and $Y_{A_s=69}/Y_{A_s=63}$ (diamonds).

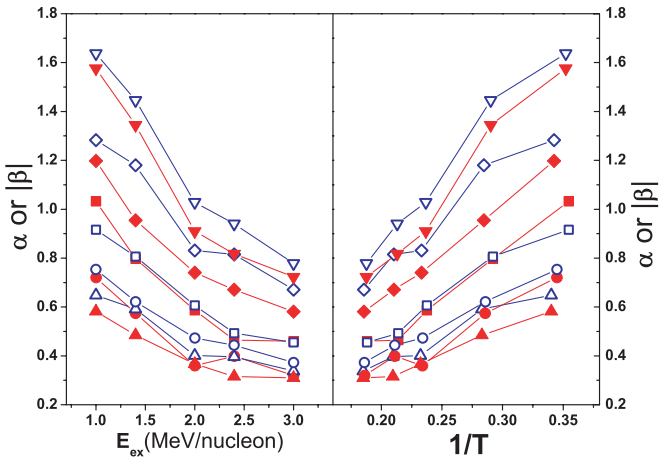

FIG. 5. (Color online) Same as Fig. 4, but for various source pairs with $Z_s = 50$. Symbols in the figure are α (solid symbols) or $|\beta|$ (open symbols) from source pair $Y_{A_s=105}/Y_{A_s=100}$ (squares), $Y_{A_s=110}/Y_{A_s=105}$ (circles), $Y_{A_s=115}/Y_{A_s=110}$ (up-triangles), $Y_{A_s=110}/Y_{A_s=100}$ (down-triangles), and $Y_{A_s=115}/Y_{A_s=105}$ (diamonds).

Both parameters α and $|\beta|$ in Figs. 4 and 5 have monotonic dependence on the excitation energy and their absolute values decrease with the excitation energy, $|\beta|$ generally are greater than α. In right panel of Figs. 4 and 5, α and $|\beta|$ show linear dependence on $1/T$, which evidences the relationship of $\alpha = \Delta\mu_n/T$ and $\beta = \Delta\mu_p/T$ [21]. The slope of the relation between α ($|\beta|$) and $1/T$ should be the free neutron (proton) chemical potential difference $\Delta\mu_n$ ($|\Delta\mu_p|$), the linear dependence of α ($|\beta|$) on $1/T$ also evidences the constant of free neutron (proton) chemical potential difference $\Delta\mu_n$ ($|\Delta\mu_p|$) between two initial sources with defined asymmetry

TABLE I. Level density parameters a_T and temperature T for different source systems and excitation energies.

Source	E_{ex} (MeV)	a_T	T (MeV)[a]
$Z_s = 30$, $A_s = 60/63$	1.0	7.5/7.8	2.8/2.9
	1.4	7.3/7.6	3.4/3.5
	2.0	7.1/7.4	4.1/4.2
	2.4	7.0/7.3	4.5/4.6
	3.0	6.8/7.1	5.1/5.2
$Z_s = 30$, $A_s = 66/69$	1.0	8.1/8.5	2.9/2.9
	1.4	8.0/8.3	3.5/3.5
	2.0	7.7/8.0	4.2/4.2
	2.4	7.6/7.8	4.6/4.7
	3.0	7.4/7.6	5.2/5.3
$Z_s = 50$, $A_s = 100/105$	1.0	11.8/12.3	2.8/2.9
	1.4	11.5/11.9	3.4/3.5
	2.0	11.0/11.4	4.2/4.3
	2.4	10.8/11.2	4.6/4.7
	3.0	10.5/10.9	5.3/5.4
$Z_s = 50$, $A_s = 110/115$	1.0	12.8/13.2	2.9/3.0
	1.4	12.4/12.8	3.5/3.6
	2.0	11.9/12.3	4.3/4.3
	2.4	11.6/12.0	4.8/4.8
	3.0	11.3/11.8	5.4/5.4

[a]Refers to the saddle-point configuration temperature.

TABLE II. Difference of free neutron and proton chemical potential $\mu_{nI} - \mu_{pI}$ for series isospin asymmetry systems from the slope fitting in Figs. 4 and 5.

System Z_s A_{s_1} A_{s_2}	$\Delta\mu_n$[a] (MeV)	$\Delta\mu_p$[b] (MeV)	$\mu_n - \mu_p$[c] (MeV)
30 60 63	2.79 ± 0.21	3.42 ± 0.33	6.21 ± 0.39
30 63 66	2.94 ± 0.29	3.53 ± 0.30	6.47 ± 0.42
30 66 69	1.64 ± 0.24	2.42 ± 0.53	4.06 ± 0.58
30 60 66	5.38 ± 0.23	5.77 ± 0.49	11.25 ± 0.54
30 63 69	4.35 ± 0.20	4.71 ± 0.22	9.06 ± 0.30
50 100 105	3.66 ± 0.28	2.96 ± 0.29	6.62 ± 0.40
50 105 110	2.58 ± 0.35	2.40 ± 0.10	4.98 ± 0.36
50 110 115	1.89 ± 0.15	2.13 ± 0.29	4.02 ± 0.33
50 100 110	5.53 ± 0.48	5.41 ± 0.49	10.94 ± 0.69
50 105 115	3.95 ± 0.11	4.06 ± 0.53	8.01 ± 0.54

[a]Refers to $\mu_{n,A_{s_2}} - \mu_{n,A_{s_1}}$.
[b]Refers to $\mu_{p,A_{s_2}} - \mu_{p,A_{s_1}}$.
[c]Refers to $(\mu_{n,A_{s_2}} - \mu_{p,A_{s_2}}) - (\mu_{n,A_{s_1}} - \mu_{p,A_{s_1}})$.

isospin, which are independent of the excitation energy or temperature. The linear dependence of isoscaling parameters α and β with $1/T$ offers a signal to calculate the free neutron (proton) chemical difference $\Delta\mu_n$ ($|\Delta\mu_p|$), which can be calculated from the slope fitting in the right panels of Figs. 4 and 5. Considering $\alpha > 0$ and $\beta < 0$, the free neutron (proton) chemical potential difference $\Delta\mu_n > 0$ and $\Delta\mu_p < 0$.

For an isospin asymmetry system $I = (N - Z)/A$, its neutron and proton chemical potentials are $\mu_{n,I}$ and $\mu_{p,I}$, respectively. From the isoscaling calculation we can get the free neutron and proton chemical potential differences $\Delta\mu_n = \mu_{n,I_2} - \mu_{n,I_1}$ and $\Delta\mu_p = \mu_{p,I_2} - \mu_{p,I_1}$, thus $\Delta\mu_n - \Delta\mu_n = (\mu_{n,I_2} - \mu_{n,I_1}) - (\mu_{p,I_2} - \mu_{p,I_1})$. If one isospin symmetry system with $I = 0$ is included, $\mu_{n,I=0} = \mu_{p,I=0}$, the difference of free neutron and proton chemical potential $\mu_{nI} - \mu_{pI}$ of the isospin asymmetry system can be deduced as shown in [13,19]. This $\mu_{nI} - \mu_{pI}$ extracted from Figs. 4 and 5 are printed in Table II, in which the index of isospin asymmetry parameter I was replaced by the mass number A_s.

B. Dependences of α and β on isospin asymmetry and source size

To explore the origin of isoscaling behavior and the dependence of isoscaling parameters α and β on the system size and the isospin composition, we performed calculations on source systems with different sizes and asymmetry (N_s/Z_s) values. The symmetry energy coefficient C_{sym} is dependent on not only the nuclear density ρ, but also the system temperature [44]. In the GEMINI investigation, the nuclear density is set to be around the saturation density ρ_0 so that the system density influences on the extraction of symmetry energy coefficient can be neglected in this case. The symmetry energy coefficient C_{sym} can be seen only as temperature dependent. Since the systems have different sizes, the temperatures of the system are slightly different even though the excitation energy is fixed at same values. In this case, in Figs. 6 and 7 the temperature is served as a correction factor, we made the temperature correction by $\alpha \cdot T$ and $\beta \cdot T$. Figures 6 and 7 depict $\alpha \cdot T$

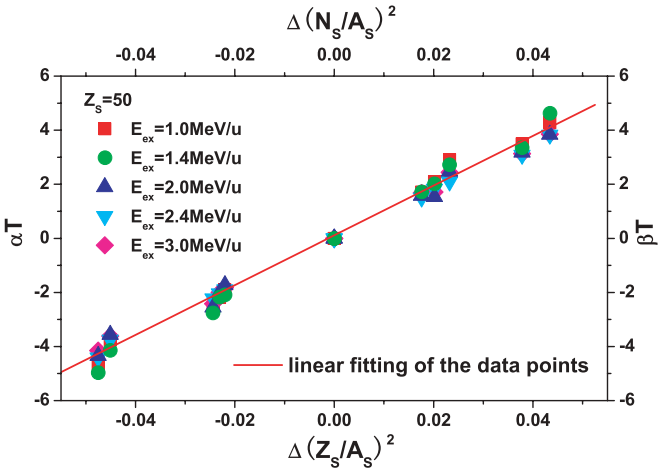

FIG. 6. (Color online) $\alpha \cdot T$ (positive parts) and $\beta \cdot T$ (negative parts) as a function of $(Z_s/A_s)_1^2 - (Z_s/A_s)_2^2$ or $(N_s/A_s)_1^2 - (N_s/A_s)_2^2$ of the sources for various source pairs with atomic number $Z_s = 50$ which is illustrated in the figure at different excitation energies.

as a function of $(Z_s/A_s)_1^2 - (Z_s/A_s)_2^2$ and $\beta \cdot T$ as a function of $(N_s/A_s)_1^2 - (N_s/A_s)_s^2$ of the initial source pair, plotted in the same figure for different excitation energies. The source pairs we simulated are $Z_s = 50$ pairs ($Z_s = 50$: $A_s = 100$, 105, 110, and 115) and $Z_s = 30$ pairs ($Z_s = 30$: $A_s = 60$, 63, 66, and 69). All these systems with different source sizes and isospin asymmetries lie along one line, which illustrates that the isoscaling parameters α and β are not sensitive to the system size and charge. The linear fits of the calculation points in Figs. 6 and 7 are printed in the figures, slopes in Fig. 6 are 92.0 ± 2.8 and 95.0 ± 1.6 in Fig. 7, respectively. This approximate linear relationship has been also observed in many experimental data [12,13] as well as other model calculations with the EES, SMM model [21], AMD [15], and IQMD model [26].

It has been shown in the framework of the grand-canonical limit of the statistical multifragmentation model [21] and

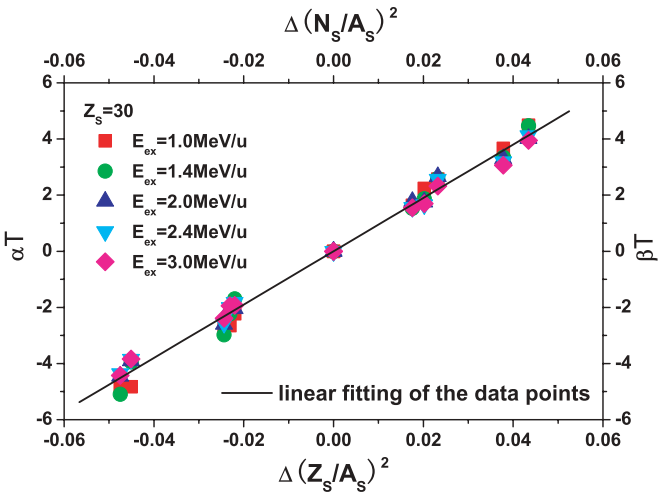

FIG. 7. (Color online) Same as Fig. 6, but for various source pairs with $Z_s = 30$ which is illustrated in the figure at different excitation energies.

in the expanding-emitting source model [13] that a simple relationship can be derived between isoscaling parameters α and $\Delta(Z_s/A_s)^2$, β and $\Delta(N_s/A_s)^2$ of the sources by following forms:

$$\alpha = 4\frac{C_{sym}}{T}\left[\left(\frac{Z_s}{A_s}\right)_1^2 - \left(\frac{Z_s}{A_s}\right)_2^2\right] \tag{10}$$

and

$$\beta = 4\frac{C_{sym}}{T}\left[\left(\frac{N_s}{A_s}\right)_1^2 - \left(\frac{N_s}{A_s}\right)_2^2\right]. \tag{11}$$

The above equations have been proven to be good approximations by many calculations and experimental data, and are generally adopted to constrain the symmetry energy coefficient C_{sym} in experiment. Here they are verified by the results in Figs. 6 and 7, i.e., the slope of $\alpha \cdot T$ with respect to $\Delta(Z_s/A_s)^2$ and $\beta \cdot T$ with respect to $\Delta(N_s/A_s)^2$. By linearly fitting the data in Figs. 6 and 7 with Eqs. (10) and (11), the symmetry energy coefficient C_{sym} can be constrained to be 23.0 ± 0.7 MeV from Fig. 6 and 23.8 ± 0.4 MeV from Fig. 7, comparable with the values from other models and experiments [12,13,15,21].

IV. SURFACE CONTRIBUTION TO ISOSPIN EFFECT

The GEMINI code involves the isospin effect or symmetry energy in calculating the binding energy. For heavy systems ($Z_s > 12$), the mass excess of the initial and residual systems of a spherical nucleus is given by the following equation [38,39]:

$$\begin{aligned} M_{macro}^{(0)} &= M_n N + M_p Z - a_v(1 - k_v I^2)A + a_s(1 - k_s I^2) \\ &\times \left\{ A^{2/3} - 3\left(\frac{a}{r_0}\right)^2 + \left(\frac{r_0}{a}A^{1/3} + 1\right) \right. \\ &\times \left. \left[2A^{2/3} + 3\frac{a}{r_0}A^{1/3} + 3\left(\frac{a}{r_0}\right)^2 \right] e^{2r_0 A^{1/3}/a} \right\} \\ &+ \frac{3}{5}\frac{e^2}{r_0}\left[\frac{Z^2}{A^{1/3}} - \frac{5}{2}\left(\frac{b}{r_0}\right)^2\frac{Z^2}{A} - \frac{5}{4}\left(\frac{3}{2\pi}\right)^{2/3}\frac{Z^{4/3}}{A^{1/3}}\right] \\ &+ W(|I| + d) - a_{el}Z^{2.39} \\ &+ \begin{cases} \Delta - \frac{1}{2}\delta, & N \text{ and } Z \text{ odd} \\ \frac{1}{2}\delta, & N \text{ or } Z \text{ odd} \\ -(\Delta - \frac{1}{2}\delta), & N \text{ and } Z \text{ even} \end{cases} \end{aligned} \tag{12}$$

where $I = (N - Z)/A$. The parameters are taken from [39], $M_n = 8.071431$, $M_p = 7.289034$, $e^2 = 1.4399764$, $b = 0.99$, $W = 36$, $a_{el} = 1.433e^{-5}$, $r_0 = 1.16$, $a = 0.68$, $a_s = 21.13$, $k_s = 2.3$, $a_v = 15.9937$, $k_v = 1.927$, $\Delta = 12/\sqrt{A}$, $\delta = 20/A$. The correction arising from single-particle effect is added to Eq. (12), which includes the Coulomb energy for diffusive surface, proton form factor, and charge asymmetry term [38,39,43]. In the top panel of Fig. 8, the mass excess calculated by Eq. (12) is plotted as a function of mass number A, the isotopes with different charge number Z from 5 to 60 are presented by lines from left to right.

In Eq. (12) the dominant symmetry energy term arises from two parts: the volume symmetry energy part $a_v k_v I^2 A$ and the

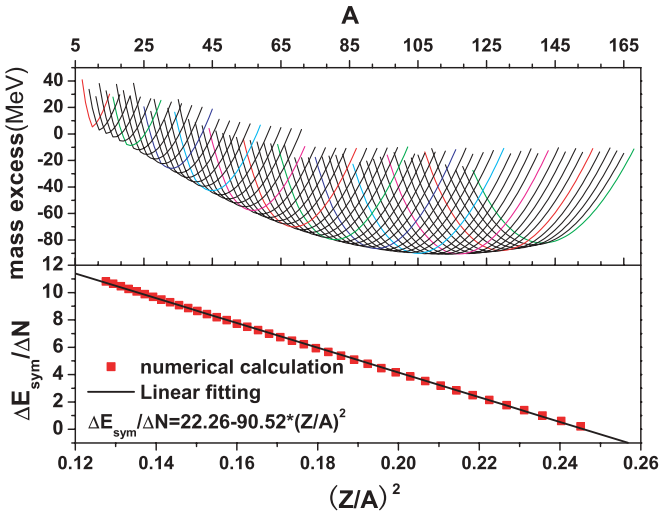

FIG. 8. (Color online) Top panel: mass excess calculated from Eq. (12) as a function of nuclear mass number, curves from left to right correspond to the atomic number Z of isotopes series from $Z = 5$ to $Z = 60$ in order. Bottom panel: numerically calculated derivative of symmetry energy E_{sym} (MeV/nucleon) with respect to neutron number N in Eq. (12) as a function of $(Z/A)^2$ (solid marks) and the linear fit of the numerical calculation, fitted result is printed in the figure.

surface diffuseness term related with the isospin asymmetry $-a_s k_s I^2\{A^{2/3} + \cdots\}$. As derived in other models and the theoretical frame [8,21], the isotope yield ratio is dominantly determined by the symmetry term in the binding energy for two equilibrium sources with comparable mass and temperature but different isospin degree N_s/Z_s. In this case, the isoscaling parameter α can be achieved by the following approximate form:

$$\alpha = -\Delta s_n / T, \tag{13}$$

where Δs_n is the difference in neutron separation energy between the two sources, considering the dominant term in separation energy is symmetry term, which is calculated in the GEMINI simulation by Eq. (13). The symmetry term taken from Eq. (13) can be expressed alone by

$$E_{sym} = c_v I^2 A - c_s I^2\{A^{2/3} + \cdots\}, \tag{14}$$

the first term in Eq. (14) is the volume term of the isospin asymmetry part, the second term is the surface effect of isospin asymmetry. $c_v = a_v k_v = 15.9937 \times 1.927 = 30.8199$ MeV which is the generally used symmetry energy coefficient at saturate nuclear density $\rho_0 = 0.16$ fm^{-3}, $c_s = a_s k_s = 21.13 \times 2.3 = 48.599$ MeV. The difference in neutron separation energy between two sources can be approximately obtained by taking the derivatives of the symmetry energy of Eq. (14) with respect to N. A numerical calculation of the derivatives of Eq. (14) with respect to N (i.e., $\Delta E_{sym}/\Delta N$) is performed, and an approximate linear function on $(Z/A)^2$ is observed, shown in the bottom panel of Fig. 8. The linear fits give $\Delta E_{sym}/\Delta N = 22.26019 - 90.5205(Z/A)^2 \approx 22.63(1 - 4(Z/A)^2)$, effective symmetry energy coefficient C_{sym} in the equation of state deduced here approximates 22.63 MeV, which is consistent with the symmetry energy coefficient C_{sym} derived from isoscaling parameters α and β very well, namely, $C_{sym} = 23.0 \pm 0.7$ MeV derived from α or $C_{sym} = 23.8 \pm 0.4$ MeV from β. As we know, the derivatives with respect to N of the volume term in Eq. (14) are $c_v(1 - 4(Z/A)^2) = 30.8199 - 123.2796(Z/A)^2 = 30.8199(1 - 4(Z/A)^2)$, hence the contribution from the surface effect is approximately $22.630125(1 - 4(Z/A)^2) - 30.8199(1 - 4(Z/A)^2) = -8.55971(1 - 4(Z/A)^2)$. The sum of the volume and surface terms of the symmetry energy gives the consistent result with the experimental results [21] and other model calculations, which indicates that the surface effect term of the symmetry energy strongly influences the isoscaling parameters α and β.

V. SUMMARY

The statistical sequential decay process of the equilibrated source has been successfully investigated by the GEMINI model. The model constrains the source size and fragments density at saturate nuclear density ρ_0 and the decay starts from an equilibrated system which is separated from any dynamical process. By only calculating the first step decay, the source size, density, and temperature can be well defined. In our work we apply it to survey the evolution of the isospin degree of freedom. Isospin effects on the decayed fragments from different source sizes, isospin asymmetries, and excitation energies have been systematically investigated. Isoscaling phenomena are observed for the emission fragments of light fragments. Isoscaling parameters α and $|\beta|$ decrease with the increase of excitation energy, they generally show linear dependence on the inverse of the system temperature T, and are independent of the source size. From the linear function between α versus $1/T$ or β versus $1/T$, the extracted linear slope is the free neutron (proton) chemical potential difference $\Delta\mu_n$ and $\Delta\mu_p$ between two systems. If the isospin symmetry source is included, then the difference of neutron and proton chemical potential $\Delta\mu_n - \Delta\mu_p$ can be determined, thus the slope difference between α and β versus $1/T$ offers a signal to calculate the neutron and proton chemical potential difference. After considering the system temperature, the simple relationship $\alpha = 4C_{sym}[(Z_1/A_1)^2 - (Z_2/A_2)^2]/T$ and $\beta = 4C_{sym}[(N_1/A_1)^2 - (N_2/A_2)^2]/T$ can be well reproduced for various sources. Only when the surface effect term in the symmetry energy is taken into account, the above linear relationship between α and $\Delta(Z/A)_s^2$, or β and $\Delta(N/A)_s^2$ can give a consistent symmetry energy coefficient C_{sym} with experimentally proposed results and other model results, which illustrates that the surface effect plays a significant role in the symmetry energy term.

ACKNOWLEDGMENTS

This work was supported in part by the National Natural Science Foundation of China under Grant Nos. 10405033, 10505026, 10405032, 10535010, 10610285, the Shanghai Development Foundation for Science and Technology under Grant Nos. 05XD14021 and 06JC14082, the Knowledge Innovation Project of Chinese Academy of Sciences

under Grant No. KJXC3-SYW-N2, Agreement of Scientific Cooperation between China and Slovakia by Ministry of Sciences and Technology the Major State Basic Research Development Program under contract No. 2007CB815004.

[1] M. Di Toro, V. Baran, M. Colonna, G. Fabbri, A. B. Larionov, S. Maccarone, and L. Scalone, Prog. Part. Nucl. Phys. **42**, 125 (1999), and references therein.
[2] B. A. Li, C. M. Ko, and W. Bauer, Int. J. Mod. Phys. E **7**, 147 (1998), and references therein.
[3] Y. G. Ma, Q. M. Su, W. Q. Shen, D. D. Han, J. S. Wang, X. Z. Cai, D. Q. Fang, and H. Y. Zhang, Phys. Rev. C **60**, 024607 (1999).
[4] H. Müller and B. D. Serot, Phys. Rev. C **52**, 2072 (1995).
[5] I. Bombaci, T. S. Kuo, and U. Lombardo, Phys. Rep. **242**, 165 (1994).
[6] S. Das Gupta, A. Z. Mekjian, and M. B. Tsang, Adv. Nucl. Phys. **26**, 91 (2001).
[7] H. S. Xu, M. B. Tsang, T. X. Liu, X. D. Liu, W. G. Lynch, W. P. Tan, A. Vander Molen, G. Verde, A. Wagner, H. F. Xi, C. K. Gelbke, L. Beaulieu, B. Davin, Y. Larochelle, T. Lefort, R. T. de Souza, R. Yanez, V. E. Viola, R. J. Charity, and L. G. Sobotka, Phys. Rev. Lett. **85**, 716 (2000).
[8] M. B. Tsang, W. A. Friedman, C. K. Gelbke, W. G. Lynch, G. Verde, and H. S. Xu, Phys. Rev. Lett. **86**, 5023 (2001).
[9] J. Brzychczyk, D. S. Bracken, K. Kwiatkowski, K. B. Morley, E. Renshaw, and V. E. Viola, Phys. Rev. C **47**, 1553 (1993).
[10] V. Volkov, Phys. Rep. **44**, 93 (1978).
[11] M. Veselsky, G. A. Souliotis, and M. Jandel, Phys. Rev. C **69**, 044607 (2004).
[12] G. A. Souliotis, D. V. Shetty, M. Veselsky, G. Chubarian, L. Trache, A. Keksis, E. Martin, and S. J. Yennello, Phys. Rev. C **68**, 024605 (2003).
[13] A. S. Botvina, O. V. Lozhkin, and W. Trautmann, Phys. Rev. C **65**, 044610 (2002).
[14] E. Geraci, M. Bruno, M. D'Agostino, E. De Filippo, A. Pagano, G. Vannini, M. Alderighi, A. Anzalone, L. Auditore, V. Baran, R. Barnà, M. Bartolucci, I. Berceanu, J. Blicharska, A. Bonasera, B. Borderie, R. Bougault, J. Brzychczyk, G. Cardella, S. Cavallaro, A. Chbihi, J. Cibor, M. Colonna, D. De Pasquale, M. Di Toro, F. Giustolisi, A. Grzeszczuk, P. Guazzoni, D. Guinet, M. Iacono-Manno, A. Italiano, S. Kowalski, E. La Guidara, G. Lanzalone, G. Lanzaó, N. Le Neindre, S. Li, S. Lo Nigro, C. Maiolino, Z. Majka, G. Manfredi, T. Paduszynski, M. Papa, M. Petrovici, E. Piasecki, S. Pirrone, G. Politi, A. Pop, F. Porto, M. F. Rivet, E. Rosato, S. Russo, P. Russotto, G. Sechi, V. Simion, M. L. Sperduto, J. C. Steckmeyer, A. Trifirò, M. Trimarchi, M. Vigilante, J. P. Wieleczko, J. Wilczynski, H. Wu, Z. Xiao, L. Zetta, and W. Zipper, Nucl. Phys. **A732**, 173 (2004).
[15] D. V. Shetty, S. J. Yennello, A. S. Botvina, G. A. Souliotis, M. Jandel, E. Bell, A. Keksis, S. Soisson, B. Stein, and J. Iglio, Phys. Rev. C **70**, 011601(R) (2004).
[16] A. Le Fèvre, G. Auger, M. L. Begemann-Blaich, N. Bellaize, R. Bittiger, F. Bocage, B. Borderie, R. Bougault, B. Bouriquet, J. L. Charvet, A. Chbihi, R. Dayras, D. Durand, J. D. Frankland, E. Galichet, D. Gourio, D. Guinet, S. Hudan, G. Immé, P. Lautesse, F. Lavaud, R. Legrain, O. Lopez, J. Lukasik, U. Lynen, W. F. J. Müller, L. Nalpas, H. Orth, E. Plagnol, G. Raciti, E. Rosato, A. Saija, C. Schwarz, W. Seidel, C. Sfienti, B. Tamain, W. Trautmann, A. Trzciński, K. Turzó, E. Vient, M. Vigilante, C. Volant, B. Zwiegliński, and A. S. Botvina, Phys. Rev. Lett. **94**, 162701 (2005).
[17] J. Iglio, D. V. Shetty, S. J. Yennello, G. A. Souliotis, M. Jandel, A. L. Keksis, S. N. Soisson, B. C. Stein, S. Wuenschel, and A. S. Botvina, Phys. Rev. C **74**, 024605 (2006) .
[18] S. Kowalski, J. B. Natowitz, S. Shlomo, R. Wada, K. Hagel, J. Wang, T. Materna, Z. Chen, Y. G. Ma, L. Qin, A. S. Botvina, D. Fabris, M. Lunardon, S. Moretto, G. Nebbia, S. Pesente, V. Rizzi, G. Viesti, M. Cinausero, G. Prete, T. Keutgen, Y. El Masri, Z. Majka, and A. Ono, Phys. Rev. C **75**, 014601 (2007).
[19] V. Baran, M. Colonna, V. Greco, and M. Di Toro, Phys. Rep. **410**, 335 (2005).
[20] M. B. Tsang, W. A. Friedman, C. K. Gelbke, W. G. Lynch, G. Verde, and H. S. Xu, Phys. Rev. C **64**, 041603(R) (2001).
[21] M. B. Tsang, C. K. Gelbke, X. D. Liu, W. G. Lynch, W. P. Tan, G. Verde, H. S. Xu, W. A. Friedman, R. Donangelo, S. R. Souza, C. B. Das, S. Das Gupta, and D. Zhabinsky, Phys. Rev. C **64**, 054615 (2001).
[22] K. Wang, Ma Yu-Gang, Wei Yi-Bin, Cai Xiang-Zhou, Chen Jin-Gen, Fang De-Qing, Guo Wei, Ma Guo-Liang, Shen Wen-Qing, Tian Wen-Dong, Zhong Chen, and Zhou Xing-Fei, Chin. Phys. Lett. **22**, 53 (2005).
[23] Y. G. Ma, K. Wang, X. Z. Cai, J. G. Chen, J. H. Chen, D. Q. Fang, W. Guo, C. W. Ma, G. L. Ma, W. Q. Shen, Q. M. Su, W. D. Tian, Y. B. Wei, T. Z. Yan, C. Zhong, X. F. Zhou, and J. X. Zuo, Phys. Rev. C **72**, 064603 (2005).
[24] Y. G. Ma, K. Wang, Y. B. Wei, G. L. Ma, X. Z. Cai, J. G. Chen, D. Q Fang, W. Guo, W. Q. Shen, W. D. Tian, and C. Zhong, Phys. Rev. C **69**, 064610 (2004).
[25] A. Ono, P. Danielewicz, W. A. Friedman, W. G. Lynch, and M. B. Tsang, Phys. Rev. C **68**, 051601(R) (2003).
[26] W. D. Tian, Ma Yu-Gang, Cai Xiang-Zhou, Chen Jin-Gen, Chen Jin-Hui, Fang De-Qing, Guo Wei, Ma Chun-Wang, Ma Guo-Liang, Shen Wen-Qing, Wang Kun, Wei Yi-Bin, Yan Ting-Zhi, Zhong Chen, and Zuo Jia-Xu, Chin. Phys. Lett. **22**, 306 (2005).
[27] Ad. R. Raduta, Eur. Phys. J. A **24**, 85 (2005).
[28] C. O. Dorso, Phys. Rev. C **73**, 034605 (2006).
[29] C. Zhong, Ma Yu-Gang, Fang De-Qing, Cai Xiang-Zhou, Chen Jin-Gen, Shen Wen-Qing, Tian Wen-Dong, Wang Kun, Wei Yi-Bin, Chen Jin-Hui, Guo Wei, Ma Chun-Wang, Ma Guo-Liang, Su Qian-Min, Yan Ting-Zhi, and Zuo Jia-Xu, Chin. Phys. **15**, 1481 (2006).
[30] W. D. Tian, Y. G. Ma, X. Z. Cai, D. Q. Fang, W. Guo, C. W. Ma, G. H. Liu, W. Q. Shen, Y. Shi, H. W. Wang, K. Wang, W. Xu, and T. Z. Yan, nucl-th/0601079.
[31] D. Q. Fang, Y. G. Ma, C. Zhong, C. W. Ma, X. Z. Cai, J. G. Chen, J. H. Chen, W. Guo, G. L. Ma, W. D. Tian, K. Wang, T. Z. Yan, J. X. Zuo, and W. Q. Shen, nucl-th/0601067.
[32] M. Colonna and M. B. Tsang, Eur. Phys. J. A **30**, 165 (2006).
[33] R. J. Charity, M. A. McMahan, G. J. Wozniak, R. J. McDonald, L. G. Moretto, D. G. Sarantites, L. G. Sobotka, G. Guarino, A. Pantaleo, L. Fiore, A. Gobbi, and K. D. Hildenbrand, Nucl. Phys. **A483**, 371 (1988).

[34] R. J. Charity, computer code GEMINI, see http://www.chemistry.wustl.edu/∼rc
[35] R. J. Charity, M. Korolija, D. G. Sarantites, and L. G. Sobotka, Phys. Rev. C **56**, 873 (1997).
[36] H. Hauser and H. Feshbach, Phys. Rev. **87**, 366 (1952).
[37] L. G. Moretto, Nucl. Phys. **A247**, 211 (1975).
[38] H. J. Krappe, J. R. Nix, and A. J. Sierk, Phys. Rev. C **20**, 992 (1979).
[39] P. Möller and J. R. Nix, Nucl. Phys. **A361**, 117 (1981).
[40] J. P. Lestone, Phys. Rev. C **52**, 1118 (1995).
[41] P. Donati, P. M. Pizzochero, P. F. Bortignon, and R. A. Broglia, Phys. Rev. Lett. **72**, 2835 (1994).
[42] R. J. Charity, Phys. Rev. C **58**, 1073 (1998).
[43] K. T. R. Davies and J. R. Nix, Phys. Rev. C **14**, 1977 (1976).
[44] Bao-An Li and Lie-Wen Chen, Phys. Rev. C **74**, 034610 (2006).
[45] M. Veselsky, Phys. Rev. C **74**, 054611 (2006).